

CORNER EFFECTS ON THE HYGROTHERMAL PERFORMANCE OF BUILDINGS

Gerson H. dos Santos¹ and Nathan Mendes²

¹Universidade Tecnológica Federal do Paraná – UTFPR
Department of Mechanical Engineering – 84016-260 – Ponta Grossa, Brazil
gsantos@utfpr.br

²Universidade Católica do Paraná - PUCPR.
Department of Mechanical Engineering – 80215-901 – Curitiba, Brazil

ABSTRACT

Multidimensional effects through porous building elements is barely explored in the literature due to many difficulties such as modeling complexity, computer run time, numerical convergence and highly moisture-dependent properties. Furthermore, when the multidimensional effect is considered, thermal bridges may play an important role on the hygrothermal building performance due to local increase of heat and mass flux densities. Therefore, in order to analyze the effects of building lower and upper corners, a multidimensional model has been developed to calculate the coupled heat, air and moisture transfer through building envelopes. For improving the discretized model numerical stability, the algebraic equations are simultaneously solved for the three driving potentials: temperature, vapor pressure and gas pressure gradients. In the results section, the coupling of the upper corner, wall, lower corner, ground and floor are analyzed for different boundary conditions in terms of temperature and relative humidity profiles, vapor flow and heat flux, showing the importance of a detailed hygrothermal analysis for accurately predicting building energy consumption, thermal comfort and mould growth risk.

INTRODUCTION

Residential, commercial and public buildings are greatly responsible for the total consumption of electricity, in a worldwide context. Only considering Brazil, they are responsible for at least 45%, which progressively motivates energy conservation studies for promoting building energy efficiency. In this context, to evaluate the building performance with thermal parameters, several codes have been developed. However, most of those codes do not take into account the moisture presence within building envelopes and the multidimensional effects. The moisture in building porous elements can imply an additional mechanism of transport absorbing or releasing latent heat of vaporization, affecting the hygrothermal building performance, causing mold growth and structural damage.

Furthermore, when the multidimensional effect is considered, thermal bridges may play an important role. Thermal bridges appear in places where the

envelope changes its geometry – such as corners and foundations - or material composition or both. Thermal bridge is used to define each part of the building envelope, where there is a local increase of heat flux density and a decrease or increase of internal surface temperatures. Beyond the thermal effect, the mass transport is also affected in the corner region and this fact is still barely explored in the literature due to modelling complexity, high computer run time, numerical divergence and highly moisture-dependent properties. However, around internal corners is where moisture can be easily accumulated, increasing mould growth risks (Fig. 1) and causing structural damage (Fig. 2).



Figure 1. Mould growth at the upper corner surface.



Figure 2. Structural damage at the lower corner surface.

In order to analyse the thermal bridge, among the first works found in the literature, Brown and Wilson (1963) verified the insulation effect with some examples and illustrated factors that influence the thermal performance of the thermal bridges. Hassid (1990) proposed a correction to the one-directional heat transfer algorithms, to account for heat transfer across thermal bridges between parallel elements.

Others authors analyzed the heat losses to the ground and the effect of perimeter insulation for the case of regular slab-on-grade foundations, such as, Hagentoft (1991), Anderson (1993) and Krarti (1993). Blomberg (1996) also developed computer programs for transient and steady-state heat conduction in two and three dimensions. These codes could be used for analyses of thermal bridge effects without moisture transport.

In soil simulations, some parameters such as boundary conditions, initial conditions, simulation time period (including warm-up), simulation time step and grid refinement have to be carefully chosen and combined in order to reach accuracy without using excessive computational processing. Beyond this analysis, Santos and Mendes (2004) verified the importance of considering a multidimensional approach for the soil domain for low-rise buildings, using a simple conductive model for ground heat transfer calculation.

Recently, Narowski *et al.* (2011) described a simple method that allows to model the conduction transfer functions for typical thermal bridges. This study was accomplished to improve building energy calculation results obtained from dynamic simulations by incorporating thermal bridges correction factors into building simulation codes.

Nevertheless, regarding moisture effects on thermal bridges, just a few research is found in the literature. Deru (2003) cited that in soils, the moisture can vary the effective thermal conductivity by a factor of ten. In his study the effects of moisture added to the ground surface and the effects of water-table depth on the heat transfer from a slab-on-grade and a basement were investigated, showing the importance of a detailed analysis of ground coupled heat transfer.

Therefore, in order to analyze the heat and moisture transfer through building lower thermal bridges, a multidimensional model has been developed to calculate the coupled heat, air and moisture transfer through building envelopes. For ensuring numerical stability in the present model, the linearized set of equations has been obtained by using the finite-volume method and the MultiTriDiagonal-Matrix Algorithm (Mendes *et al.*, 2002) to solve a 2-D HAM model to describe the physical phenomena of heat, air and mass (HAM) transfer through porous building materials. In the results section, the multidimensional effects coupled with the moisture transport in the lower thermal bridges formed by the soil, wall and floor are shown and analyzed in terms of temperature

and relative humidity profiles and vapor and heat flux through the floor. In the upper corner, the effects of a concrete beam in the temperature and relative humidity profiles are presented.

MATHEMATICAL MODEL

The model for the porous media domain has been elaborated considering the differential governing equations for moisture, air and energy balances. The transient terms of each governing equation have been written in terms of the driving potentials to take more advantage of the MTDMA (Mendes *et al.*, 2002) solution algorithm.

Moisture Transport

The moisture transport has been divided into liquid and vapor flows as shown in Eq. 1:

$$\mathbf{j} = \mathbf{j}_l + \mathbf{j}_v, \quad (1)$$

where \mathbf{j} is the density of moisture flow rate (kg/m²s), \mathbf{j}_l , the density of liquid flow rate (kg/m²s) and, \mathbf{j}_v , the density of vapor flow rate (kg/m²s).

The liquid transport calculation is based on the Darcy equation:

$$\mathbf{j}_l = K(\nabla P_{suc} - \rho_l \mathbf{g}), \quad (2)$$

where K is the liquid water permeability (s), P_{suc} , the suction pressure (Pa), ρ_l , the liquid water density (kg/m³) and \mathbf{g} the gravity (m/s²).

The capillary suction pressure can be written as a function of temperature and moisture content in the following form:

$$\nabla P_{suc} = \frac{\partial P_{suc}}{\partial T} \nabla T + \frac{\partial P_{suc}}{\partial P_v} \nabla P_v. \quad (3)$$

Similarly to the liquid flow, the vapor flow is calculated from the Fick's law based equation considering effects of both vapor pressure and air pressure driving potentials:

$$\mathbf{j}_v = -\underbrace{\delta_v \nabla P_v}_{\text{vapor diffusion}} - \rho_v \underbrace{\frac{kk_{rg}}{\mu_g} \nabla P_g}_{\text{convective vapor transport}}, \quad (4)$$

where δ_v is the vapor diffusive permeability (s), P_v , the partial water vapor pressure (Pa), ρ_v , the water vapor density (kg/m³), k , the absolute permeability (m²), k_{rg} , the gas relative permeability, μ_g , the dynamic viscosity (Pa.s) and, P_g , the gas pressure.

The water mass conservation equation can be described as:

$$\frac{\partial w}{\partial t} = -\nabla \cdot \mathbf{j}, \quad (5)$$

where w is the moisture content (kg/m³).

This moisture content conservation equation – Eq. 5 – can be written in terms of the three driving potentials as:

$$\frac{\partial w}{\partial \phi} \frac{\partial \phi}{\partial P_v} \frac{\partial P_v}{\partial t} + \frac{\partial w}{\partial \phi} \frac{\partial \phi}{\partial T} \frac{\partial T}{\partial t} = \nabla \cdot \left[\begin{array}{l} -K \frac{\partial P_{suc}}{\partial T} \nabla T - \\ \left(K \frac{\partial P_{suc}}{\partial P_v} - \delta_v \right) \nabla P_v + \\ \rho_v \frac{kk_{rg}}{\mu_g} \nabla P_g + K \rho_l \mathbf{g} \end{array} \right] \quad (6)$$

Air Transport

In the proposal model, the air transport is individually considered through the dry-air mass balance. In this way, the dry-air conservation equation can be expressed as:

$$\frac{\partial \rho_a}{\partial t} = -\nabla \cdot \mathbf{j}_a, \quad (7)$$

with the air flow calculated by the following expression:

$$\mathbf{j}_a = \underbrace{\delta_v \nabla P_v}_{\text{air diffusion}} - \rho_a \underbrace{\frac{kk_{rg}}{\mu_g} \nabla P_g}_{\text{air convection}}, \quad (8)$$

where ρ_a is the density of dry air (kg/m^3), \mathbf{j}_a , the density of dry air flow rate ($\text{kg/m}^2\text{s}$) and, P_g , the gas pressure (dry air pressure plus vapor pressure) in Pa.

Therefore, the dry air transport can be described as a function of the partial gas and vapor pressure driving potentials so that the air balance can be written as:

$$\frac{\partial \rho_a}{\partial P_g} \frac{\partial P_g}{\partial t} + \frac{\partial \rho_a}{\partial P_v} \frac{\partial P_v}{\partial t} + \frac{\partial \rho_a}{\partial T} \frac{\partial T}{\partial t} = \nabla \cdot \left(\begin{array}{l} -\delta_v \nabla P_v + \\ \rho_a \frac{kk_{rg}}{\mu_g} \nabla P_g \end{array} \right). \quad (9)$$

Heat Transport

The heat transfer can be attributed to both conductive and convective effects. The conductive transport is calculated by the Fourier's law:

$$\mathbf{q}_{\text{cond}} = -\lambda \nabla T, \quad (10)$$

while the convective transport can be written as:

$$\mathbf{q}_{\text{conv}} = \underbrace{\mathbf{j}_l c_{pl} T}_{\text{liquid flow}} + \underbrace{\mathbf{j}_a c_{pa} T}_{\text{dry air flow}} + \underbrace{\mathbf{j}_v L}_{\text{phase change}} + \underbrace{\mathbf{j}_v c_{pv} T}_{\text{vapor flow}} \quad (11)$$

where λ is the thermal conductivity (W/mK), c_{pa} , the specific heat capacity at constant pressure of the dry air (J/kgK), c_{pl} , the specific heat capacity of the water liquid (J/kgK), c_{pv} , the specific heat capacity at constant pressure of the vapor (J/kgK) and, L , the vaporization latent heat (J/kg).

The energy balance equation can be described as:

$$c_m \rho_0 \frac{\partial T}{\partial t} = -\nabla \cdot \mathbf{q}, \quad (12)$$

where c_m is the specific heat capacity of the structure (J/kgK) and ρ_0 , the density of the dry material (kg/m^3).

In this way, assuming 0°C as the reference temperature, the energy conservation equation can be written in terms of the three driving potentials as:

$$c_m \rho_0 \frac{\partial T}{\partial t} = \nabla \cdot \left(\begin{array}{l} \left(\lambda - K \frac{\partial P_{suc}}{\partial T} c_{pl} T \right) \nabla T - \\ \left(K \frac{\partial P_{suc}}{\partial P_v} c_{pl} T + \delta_v c_{pa} T - \right) \nabla P_v + \\ \delta_v (L + c_{pv} T) \\ \left(\rho_a \frac{kk_{rg}}{\mu_g} c_{pa} T + \right) \nabla P_g + \\ \left(\rho_v \frac{kk_{rg}}{\mu_g} (L + c_{pv} T) \right) \\ K \rho_l c_{pl} T \mathbf{g} \end{array} \right). \quad (13)$$

Boundary Conditions

In the dry-air conservation equation of the present model, gas pressure has been considered as a prescribed value - Dirichlet condition - at the envelope surface:

$$P_{g,\infty} = P_{g,\text{sup}}. \quad (14)$$

For the moisture flow, vapor transport is considered due to the difference between the partial vapor pressure in air and at the external and internal surfaces:

$$j = \beta_v (p_{v,\infty} - p_{v,\text{sup}}), \quad (15)$$

where j is the density of moisture flow rate ($\text{kg/m}^2\text{s}$) and β_v , the surface coefficient of water vapor transfer (s/m), calculated from the Lewis' relation.

For the heat transport convection heat transfer and phase change were considered:

$$q = h(T_\infty - T_{\text{sup}}) + \beta_v (p_{v,\infty} - p_{v,\text{sup}}) L(T), \quad (16)$$

where q is the heat flowing into the structure (W/m^2) and h the convective heat transfer coefficient ($\text{W/m}^2\text{K}$).

SOLUTION OF THE BALANCE EQUATIONS

A fully-implicit central-difference scheme has been considered for the discretization using the finite-volume method (Patankar, 1980) for the governing equations and the MTDMA to simultaneously solve the three set of equations.

Discretized Conservation Equations Solution of the Porous Element Domain

Implicit schemes demand the use of an algorithm to solve tridiagonal systems of linear equations. One of the most used is the well-known Thomas Algorithm or TDMA (TriDiagonal-Matrix Algorithm). However, for strongly-coupled equations of heat and mass transfer problems, a more robust algorithm may be necessary in order to achieve numerical stability (Mendes *et al.*, 2002).

For a physical problem represented by M dependent variables, the discretization of $M \times N$ differential equations, leads to the following system of algebraic equations,

$$\mathbf{A}_i \cdot \mathbf{x}_i = \mathbf{B}_i \cdot \mathbf{x}_{i+1} + \mathbf{C}_i \cdot \mathbf{x}_{i-1} + \mathbf{E}_i \quad (17)$$

where \mathbf{x} is a vector containing the M dependent variables T , P_v and P_g

$$\mathbf{x}_i = \begin{bmatrix} T \\ P_v \\ P_g \end{bmatrix}. \quad (18)$$

Differently from the traditional TDMA, coefficients \mathbf{A} , \mathbf{B} and \mathbf{C} are $M \times M$ matrices, in which each line corresponds to one dependent variable. The elements that do not belong to the main diagonal are the coupled terms for each conservation equation. \mathbf{E} is an M -element vector.

As MTDMA has the same essence as TDMA, it is necessary to replace Eq. (17) by relationships of the form

$$\mathbf{x}_i = \mathbf{P}_i \cdot \mathbf{x}_{i+1} + \mathbf{q}_i, \quad (19)$$

where \mathbf{P}_i is now a $M \times M$ matrix.

The use of this algorithm makes the systems of equations to be more diagonally dominant and the diagonal dominance is improved by the fact that the \mathbf{A}_i coefficients are increased at the same time the \mathbf{E}_i source terms are decreased. Therefore, the transient terms of the Eqs. 6 and 9 also were written thus to increase the diagonal dominance.

SIMULATION PROCEDURE

Due to the high computer run time, a simple physical domain was chosen as illustrated in Fig. 3. After several simulations to analyze the sensitivity of the solution method to time step and mesh size, the domain was divided into 730,000 nodes distributed on a regular Cartesian mesh. A 600-s time step was considered for all simulations. An area twice as big the one shown in the Fig. 3 was simulated (not shown), but a negligible difference on the temperature and relative humidity profiles was observed.

A 0.2-m thickness building envelope has been used. The hygrothermal properties have been obtained from the benchmark of the European project

HAMSTAD (Hagentoft, 2002) for brick (wall, roof and foundation), from Künzel *et al.* (2008) for concrete (floor and beam) and from Oliveira *et al.* (1993), for a sandy silt soil.

For representing a mild winter condition, external constant uniform values of 10 W/m²K, 278 K and 80% (humid condition) or 30% (dry condition) have been used for the convective heat transfer coefficient, temperature and relative humidity, respectively. On the other hand, for the summer condition, a temperature of 308 K was considered. The other remaining data been kept constant.

Internally, at the upper surface of the floor and right surface of the wall, constant uniform values of 3 W/m²K, 297 K and 50% have been considered for the convective heat transfer coefficient, temperature and relative humidity, respectively, for an air conditioned environment. The other surfaces have been considered adiabatic and impermeable. As initial conditions for the whole domain, temperature, relative humidity and gas pressure of 288 K, 60% (humid condition) or 40% (dry condition) and 100 kPa have been assumed in order to represent the winter conditions. For summer condition, only the initial temperature was changed to 303 K.

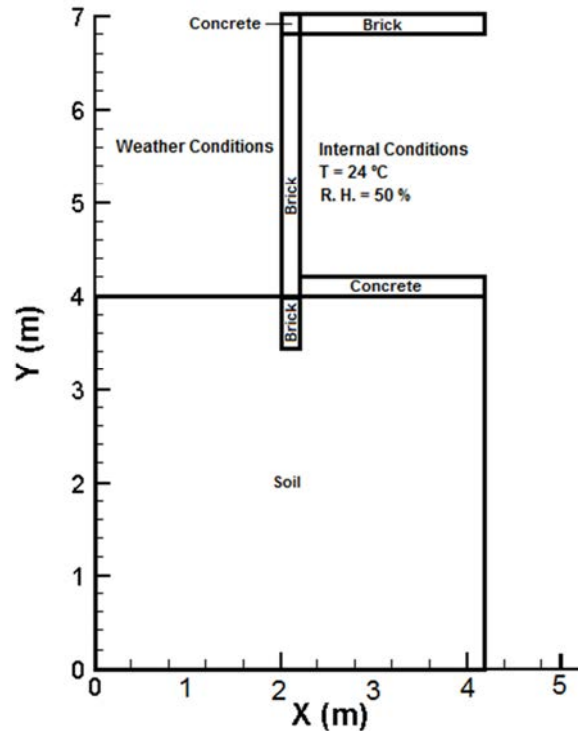


Figure 3. Physical domain of the lower and upper corners.

RESULTS

The results presented in this section illustrate the profiles of temperatures and relative humidity after one year of simulation period. Longer periods were also simulated (not showed), but the results showed only small changes in the profiles of temperature and relative humidity in the profoundness of the soil as discussed by Santos and Mendes (2005). Changes in the profiles values at the surfaces of domain and in the regions where de multidimensional effects are relevant (lower and upper corner) were negligible.

The time evolution differences on the temperature and relative humidity profiles are mainly attributed to the high thermal and hygric soil capacities. As one could expect, the temperature and relative humidity average values at deeper soil are directly associated to the yearly average magnitudes for temperature, solar radiation and partial vapor pressure.

The corner, foundation and composition material effects are observed in Figs. 4 and 5. As one can observe in these figures, the mass transport under dry and humidity climate conditions did not influence the temperature profiles. The multidimensional effect in the lower corner is noticed in a region of about 40 cm from the edge between the floor and the wall. Figure 4-D shows high values of relative humidity in this region. High values of relative humidity in the lower corner region can cause structural damage as observed in Fig. 2. High values of relative humidity are also observed in Figs. 4B and 4D in the upper corner. These values are mainly caused by material composition (concrete beam) of this region. This fact is attributed to the higher hygrothermal capacity of the concrete in comparison to the brick. This effect can increase the mould growth probability (Fig. 1) as observed by Santos and Mendes (2009).

Figure 5 showed that under hot climate conditions, the relative humidity values at the internal surface of the wall are lower than the one obtained under cold climate conditions.

Table 1 shows values of vapor and heat fluxes through the floor surface, where the minus sign indicates a downward flux, *i.e.*, outward the room. This table compares the average fluxes at the region of the corner where the multidimensional (2-D) effects are observed (40 cm from edge of the lower corner) and the 1-D case, which is the assumption employed by the great majority of building simulation codes.

As seen in Tab. 1, the latent heat flux is negligible in the total heat flux through the floor. An increased in the vapor flux was observed when a cold and dry weather condition was utilized. However, it was verified a high difference on the sensible heat flux between 1-D and 2-D models (by a factor of ten) for an air-conditioned building. This behaviour has been reported for other climatic conditions (not shown), concerning the importance of the perimeter to floor area ratio on the total heat flux.

In order to improve the mathematical model used by the building simulation code of Domus (Mendes *et al.*, 2003), a floor area of 40x40 cm along the exposed edge has been considered, increasing the heat flux (1-D floor) by a factor of ten. This change has been adopted for a typical and simple geometry as shown in Fig. 3. For other foundation configurations of, further studies should be carried out.

CONCLUSIONS

In order to analyze the effects of building lower and upper thermal bridges, a multidimensional model has been developed to calculate the coupled heat, air and moisture transfer through building envelopes.

The multidimensional effect in the lower corner was noticed in a region of about 40 cm from edge between the floor and wall. High values of relative humidity in the lower corner region were observed for cold and humid climate conditions. High values of relative humidity were also observed in the upper corner region. These values are mainly caused by material composition (concrete beam) found in this region. This fact is attributed to the higher hygrothermal capacity of the concrete in comparison to the one of brick. On the other hand, for hot climate conditions, relative humidity values at the wall internal surface are lower than those found under cold climate conditions.

Non-unidimensionality of transport phenomena the averaged heat and moisture fluxes in the corner region were also investigated. The latent heat flux was considered negligible through the floor, which is mainly attributed to the constant indoor conditions and the different time constants between temperature and moisture. It was also verified a high difference on the sensible heat flux between 1-D and 2-D models by a factor of ten. This behaviour has been also verified for other climatic conditions not shown in this paper.

It is worth remembering that the conclusions presented in this paper are limited to the simulations procedure presented in the present work, in terms of geometry, physical domain, hygrothermal properties and boundary conditions. For instance, for other foundation configurations, further research needs to be carried out as well for considering a whole building domain, under dynamic weather conditions on the thermal bridges.

ACKNOWLEDGEMENTS

The authors thank CNPq – Conselho Nacional de Desenvolvimento Científico e Tecnológico – of the Secretary for Science and Technology of Brazil, Centrais Elétricas do Brasil – ELETROBRAS and Fundação Araucária.

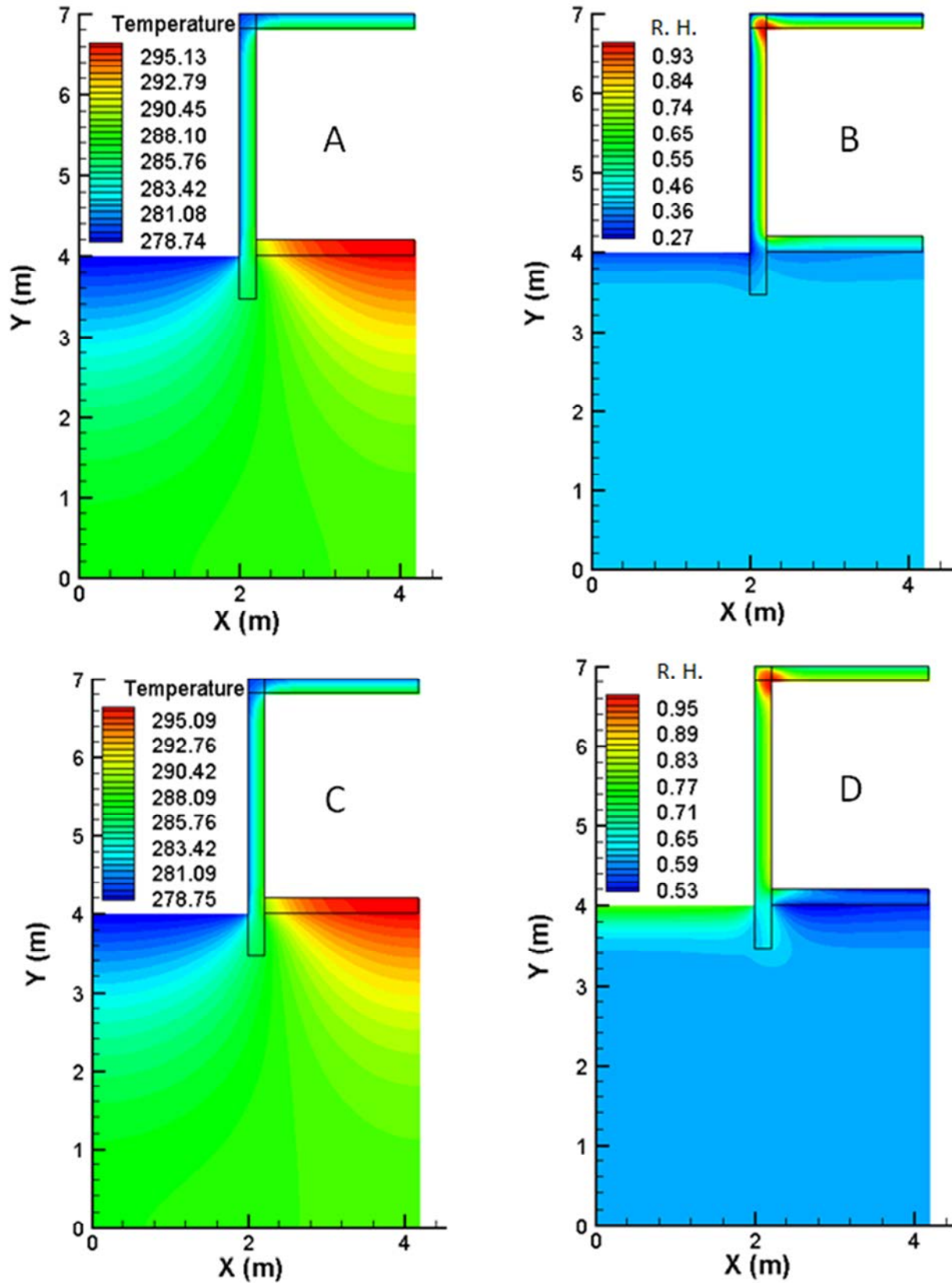


Figure 4. Temperature and relative humidity profiles for cold and dry conditions (A and B) and for cold and humidity conditions (C and D)

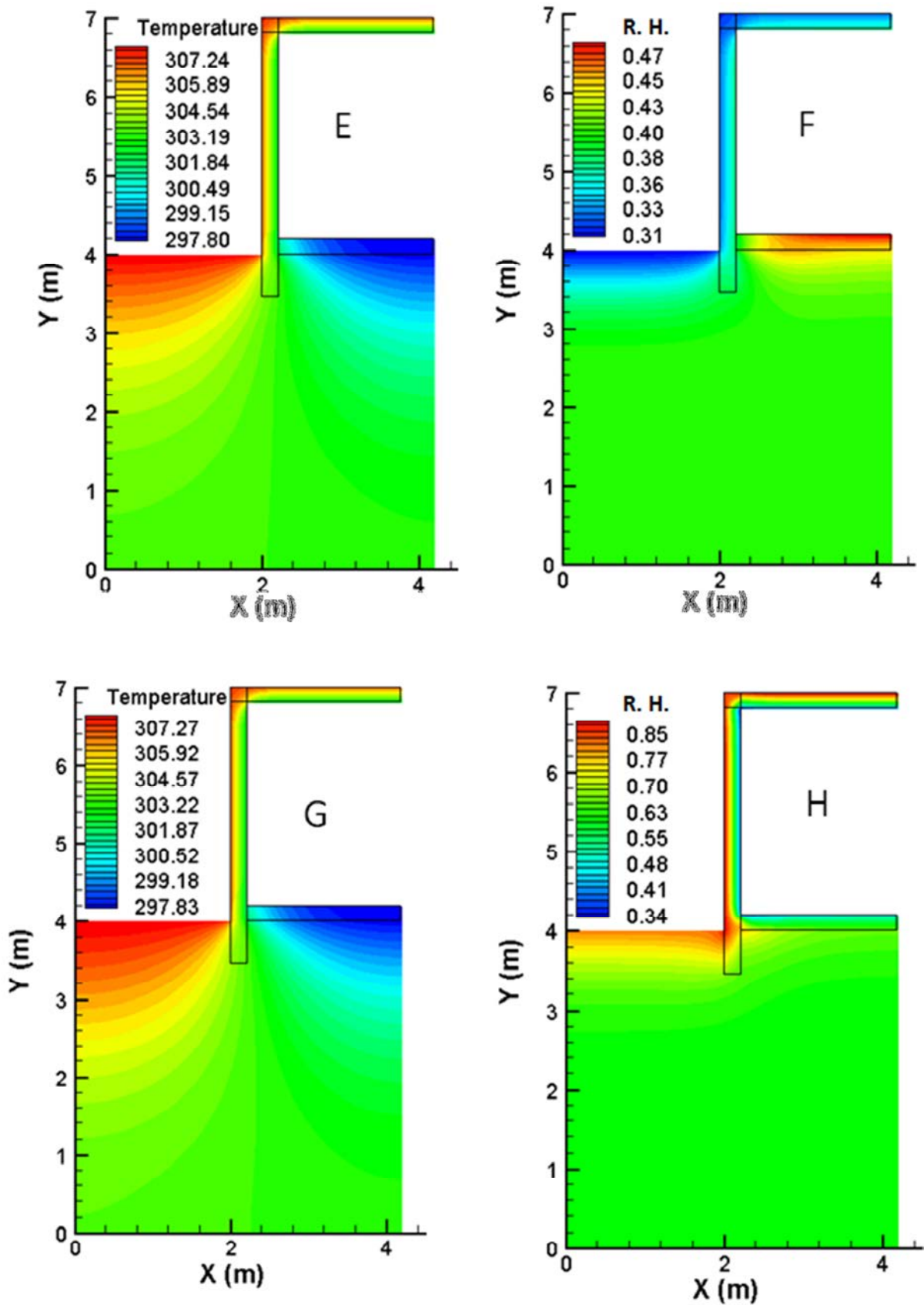


Figure 5. Temperature and relative humidity profiles for hot and dry conditions (E and F) and for hot and humidity conditions (G and H)

Table 1. Vapor and heat fluxes through the floor surface.

Condition	Vapor Flux (kg/m ² s)	Sensible Heat Flux (W/m ²)	Latent Heat Flux (W/m ²)	Total Heat Flux (W/m ²)
2-D, Cold, Moisture ignored	-	-21.07	-	-21.07
1-D, Cold, Moisture ignored	-	-2.03	-	-2.03
2-D, Cold/Dry	-2.097.10 ⁻⁷	-20.65	-0.524	-21.17
1-D, Cold/Dry	-6.107.10 ⁻⁹	-2.10	-0.015	-2.12
2-D, Cold/Humid	-6.81.10 ⁻⁸	-20.68	-0.170	-20.85
1-D, Cold/Humid	5.931.10 ⁻⁹	-2.22	0.015	-2.21
2-D, Hot/Dry	-1.158.10 ⁻⁸	12.20	-0.029	12.17
1-D, Hot/Dry	-2.458.10 ⁻⁹	1.38	-0.006	1.37
2-D, Hot/Humid	2.846.10 ⁻⁷	12.15	0.712	12.86
1-D, Hot/Humid	8.303.10 ⁻⁹	1.47	0.021	1.41

REFERENCES

- Anderson, B.R. 1993. The effect of edge insulation on the steady state heat loss through a slab-on-ground floor. *J. of Building and Environment*, Vol. 28, N. 3, pp. 361-367.
- Blomberg, T. 1996. Heat Conduction in two and three Dimensions. Computer Modelling of Building Physics Applications. Report TVBH-1008. ISBN 91-88722-05-8.
- Brown, W. P., Wilson, A. G., 1963. CBD-44. Thermal Bridges in Buildings. http://irc.nrc-cnrc.gc.ca/pubs/cbd/cbd044_e.html
- Deru, M. 2003. A Model for Ground-Coupled Heat and Moisture Transfer from Buildings. Technical Report. National Renewable Energy Laboratory.
- Hagentoft, C. E. 2002. HAMSTAD – WP2 Modeling, Report R-02:9. Gothenburg, Department of Building Physics, Chalmers University of Technology.
- Hagentoft, C.E., Claesson, J. 1991. Heat loss to the ground from a building. II: Slab on the ground. *J. of Building and Environment*, Vol. 26, N. 4, pp. 395-403.
- Hassid, S., 1990. Thermal Bridges Across Multilayer Walls: An Integral Approach. *Building and Environment*, Vol. 25, pp. 143-150.
- Krarti, M. 1993. Steady-state heat transfer from horizontally insulated slabs. *International Journal of Heat and Mass Transfer*, Vol. 36, N. 8, pp. 2135-2145.
- Künzel, H. M., Holm, A. H., Krus, M. 2008. Hygrothermal Properties and Behaviour of Concrete. *WTA-Almanach*, pp. 161-181.
- Mendes, N., Oliveira, R. C. L., Santos, G. H. 2003. Domus 2.0: A Whole-Building Hygrothermal Simulation Program. Eighth International IBPSA Conference.
- Mendes, N., Philippi, P. C., Lamberts, R. A. 2002. New Mathematical Method to Solve Highly Coupled Equations of Heat and Mass Transfer in Porous Media. *Int. Journal of Heat and Mass Transfer*, Vol. 45, pp. 509-518.
- Narowski, P., Stasiński, J., Wereszczyński, P. 2011. Modelling of Conduction transfer Functions for Typical Thermal Bridges Identified in BIM data. *Proceedings of Building Simulation 2011*, pp. 1320-1327.
- Oliveira Jr, A. A. M., Freitas, D. S., Prata, A. T. 1993. Influência das Propriedades do Meio nas Difusividades do Modelo de Phillip e de Vries em Solos Insaturados. Relatório de Pesquisa. UFSC.
- Patankar S.V. 1980. Numerical Heat Transfer and Fluid Flow, Hemisphere Publishing Corporation.
- Santos, G. H., Mendes, N. 2004. Multidimensional Effects of Ground Heat Transfer on the Dynamics of Building Thermal Performance. *ASHRAE Transactions*. Vol. 110, pp.345-354.
- Santos, G. H., Mendes, N. 2005. Unsteady Combined heat and Moisture Transfer in Unsaturated Porous Soils. *Journal of Porous Media*, Vol. 8, N. 5, pp. 493-510.
- Santos, G. H., Mendes, N. 2009. A Building Corner Model for Hygrothermal Performance and Mould Growth Risk Analyses. *International Journal of Heat and Mass Transfer*. Vol. 52, pp. 4862-4872.